Water Research 175 (2020) 115688

Contents lists available at ScienceDirect

Water Research

journal homepage: www.elsevier.com/locate/watres

A hybrid catalytic hydrogenation/membrane distillation process for nitrogen resource recovery from nitrate-contaminated waste ion exchange brine

Xiangchen Huo, Johan Vanneste, Tzahi Y. Cath, Timothy J. Strathmann*

Department of Civil and Environmental Engineering, Colorado School of Mines, Golden, CO, USA

ARTICLE INFO

Article history:
Received 10 December 2019
Received in revised form
26 February 2020
Accepted 2 March 2020
Available online 5 March 2020

Keywords:
Oxyanion
Ion exchange
Waste brine
Catalytic hydrogenation
Membrane distillation
Resource recovery

ABSTRACT

Ion exchange is widely used to treat nitrate-contaminated groundwater, but high salt usage for resin regeneration and management of waste brine residuals increase treatment costs and add environmental burdens. Development of palladium-based catalytic nitrate treatment systems for brine treatment and reuse has showed promising activity for nitrate reduction and selectivity towards the N_2 over the alternative product ammonia, but this strategy overlooks the potential value of nitrogen resources. Here, we evaluated a hybrid catalytic hydrogenation/membrane distillation process for nitrogen resource recovery during treatment and reuse of nitrate-contaminated waste ion exchange brines. In the first step of the hybrid process, a Ru/C catalyst with high selectivity towards ammonia was found to be effective for nitrate hydrogenation under conditions representative of waste brines, including expected salt buildup that would occur with repeated brine reuse cycles. The apparent rate constants normalized to metal mass (0.30 ± 0.03 mM min^{-1} g_{Ru}^{-1} under baseline condition) were comparable to the state-of-the-art bimetallic Pd catalyst. In the second stage of the hybrid process, membrane distillation was applied to recover the ammonia product from the brine matrix, capturing nitrogen as ammonium sulfate, a commercial fertilizer product. Solution pH significantly influenced the rate of ammonia mass transfer through the gas-permeable membrane by controlling the fraction of free ammonia species (NH_3) present in the solution. The rate of ammonia recovery was not affected by increasing salt levels in the brine, indicating the feasibility of membrane distillation for recovering ammonia over repeated reuse cycles. Finally, high rates of nitrate hydrogenation (apparent rate constant 1.80 ± 0.04 mM min^{-1} g_{Ru}^{-1}) and ammonia recovery (overall mass transfer coefficient 0.20 m h^{-1}) with the hybrid treatment process were demonstrated when treating a real waste ion exchange brine obtained from a drinking water utility. These findings introduce an innovative strategy for recycling waste ion exchange brine while simultaneously recovering potentially valuable nitrogen resources when treating contaminated groundwater.

1. Introduction

Over the last century, industrial N_2 fixation, enabled by the Haber-Bosch process, has played a critical role in sustaining the world's food supplies in the face of population growth. However, the process is energy-intensive and a significant fraction of nitrogen fertilizer products are released from agricultural and industrial activities and enter surface and ground waters, endangering aquatic environments and ecosystems (Camargo and Alonso, 2006). In particular, nitrate in drinking water has been recognized as a human health hazard, for which health guidelines and regulations have been established to protect populations and limit adverse effects. As a result, there has been a considerable interest in developing effective and sustainable treatment technologies for nitrate-impacted drinking water sources (Chen et al., 2019; Garcia-Segura et al., 2018; Huo et al., 2017; Martínez et al., 2017).

Ion exchange (IX) is an effective process for nitrate-contaminated groundwater documented at many drinking water treatment plants (Kapoor and Viraraghavan, 1997). One of the major challenges of using IX is brine management. Due to their finite exchange capacities, anion exchange resins (AER) require periodic regeneration using a concentrated salt brine solution (commonly sodium chloride or sodium bicarbonate). This process

* Corresponding author.
E-mail address: strthmnn@mines.edu (T.J. Strathmann).

https://doi.org/10.1016/j.watres.2020.115688
0043-1354/

consumes large quantities of salt since only a fraction of the NaCl used to prepare fresh brine solutions adsorbs to the resin during regeneration (Pintar et al., 2001). In addition, the regeneration step produces a nitrate-contaminated waste brine stream that requires disposal or further treatment (Bergquist et al., 2017a; Jensen and Darby, 2016). The low salt use efficiency and waste brine disposal are significant contributors to operation and maintenance (O&M) costs for IX treatment (Wang et al., 2011). Thus, strategies to increase salt use efficiency (i.e., percentage of the salt applied ending up on the regenerated resin) and minimize brine waste volumes are critical to improving the economics and environmental sustainability of IX processes for drinking water treatment.

Transforming nitrate to gaseous species (e.g., N_2) or aqueous species that have much lower affinity for the AER (e.g., cationic NH_4^+) can potentially enable brine recycling and minimize net salt inputs. The highly oxidized state of nitrogen in nitrate (+V) allows it to be reductively transformed, either biologically, chemically, or catalytically (Doudrick et al., 2013; Mellor et al., 1992; Wang et al., 2006; Yang and Lee, 2005; Ye et al., 2017). In recent years, catalytic hydrogenation has emerged as a promising technology for nitrate reduction, wherein supported metal catalysts, most often palladium-based bimetallic catalysts (Chen et al., 2003; Constantinou et al., 2006; Jung et al., 2014; Sá and Vinek, 2005; Xie et al., 2011), promote nitrate reduction using H_2 as a bulk reductant. Advantages of this technology include short start-up times, fast reactions, use of a clean reducing agent that can be produced renewably (H_2), low risk of bacterial contamination, and minimal production of contaminated disposals (Bergquist et al., 2016; Chen et al., 2003; Choe et al. 2013, 2015; Martínez et al., 2017; Papa et al., 2014). Many research efforts have focused on identifying catalysts and operating conditions that selectively convert nitrate to gaseous N_2 while minimizing formation of the alternative end-product ammonia. Supported bimetallic Pd catalysts (e.g., Pd−Cu, Pd−In, Pd−Sn) have been most extensively studied due to their high activity and tunable selectivity towards N_2 (Chen et al., 2003; Constantinou et al., 2006; Jung et al., 2014; Sá and Vinek, 2005; Xie et al., 2011). While generally effective for treatment of a variety of nitrate-containing water matrices, recent studies show that nitrate reactions with some catalysts can be markedly inhibited by some natural water constituents that competitively adsorb to reactive surface sites (Chaplin et al., 2006; Pintar et al., 1998; Wang et al., 2009), and reduced reaction rates for Pd−In catalysts have been documented in recent studies examining treatment of IX waste brine matrices (Bergquist et al. 2016, 2017a; Choe et al., 2015).

While catalytic nitrate reduction to gaseous N_2 eliminates nitrogen residuals from the treated water, this strategy represents a downcycling step that fails to capture any value embedded in the fixed nitrogen species present in the contaminated water. Nitrate reduction to the alternative product ammonia has typically been deemed undesirable (Bergquist et al., 2016; Dortsiou et al., 2009; Pintar et al., 2001; Yang et al., 2013), but ammonia has potential value as fertilizer products (e.g., anhydrous ammonia, ammonium sulfate) if a suitable process for recovering the endproduct can be identified (e.g., volatilization and trapping of NH_3). Opportunities for recovering ammonia are most practical in matrices where nitrate has been concentrated like IX waste brines (where nitrogen concentrations can reach >1000 mg L^{-1}) (Bae et al., 2002; McAdam and Judd, 2008; Yang et al., 2013). Thus, selective reduction of nitrate in IX waste brines to ammonia provides a potential pathway for recycling fixed nitrogen species as fertilizer products during water treatment. At the same time, removal of nitrate from the waste brine can enable reuse of the waste brine and significantly reduce net salt input requirements for the overall IX treatment processes.

In this work, we introduce a hybrid ion exchange/catalytic hydrogenation/membrane distillation (IX/CH/MD) pathway to simultaneously reduce salt input requirements and waste brine discharge volume while recovering nitrogen resources when treating nitrate-contaminated water sources (Fig. 1). Here, we focused on characterizing the waste brine management steps in the hybrid process. Specifically, we assessed (1) treatment of nitrate-contaminated IX waste brines using Ru/C, an alternative to more costly Pd-based catalysts, which we recently reported exhibits complete selectivity to ammonia when treating nitrate in freshwater matrices (Huo et al., 2017), and (2) recovery of the resulting ammonia product from brine as ammonium sulfate, a potentially valuable fertilizer product (Amaral et al., 2016; Garcia-González and Vanotti, 2015; Li et al., 2018), using membrane distillation. Experiments were conducted using both synthetic waste brine mimicking conditions reported in earlier studies as well as a real waste brine obtained from a drinking water utility that uses IX to treat nitrate-contaminated groundwater. The influence of key operating variables on the individual steps in the hybrid process were examined, and findings provide a path forward for development of the hybrid process to simultaneously enable reuse of waste IX brines and reduce waste discharges while recovering a potentially valuable product stream.

2. Materials and methods

2.1. Materials

A commercial Ru catalyst immobilized on carbon powder (Ru/C, nominal 5 wt% Ru) was purchased from Sigma-Aldrich and used as received. Previous characterization showed that the catalyst exhibits high surface area (860 $m^2 g^{-1}$) and Ru metal dispersion (38%), and H_2 temperature-programmed reduction and CO chemisorption indicate surface Ru is present predominantly in the metallic state under reaction conditions. Detailed characterization of this material was described elsewhere (Huo et al., 2017). Sodium nitrate and ammonium chloride were also obtained from Sigma-Aldrich. ACS grade sodium sulfate, sodium bicarbonate, ammonium hydroxide solution, sodium hydroxide, and hydrochloric acid were acquired from Fisher Scientific. Concentrated sulfuric acid was purchased from EMD Millipore. Ultra-high purity H_2 and CO_2 were supplied by General Air. Waste IX brine was collected from a drinking water treatment plant in California. Composition of the waste brine is summarized in Table 1.

2.2. Catalytic hydrogenation experiments

To determine the influence of operating parameters on nitrate hydrogenation reactions, kinetic studies were first conducted in synthetic brine solutions using a procedure adapted from a previous study (Huo et al., 2017). A predetermined mass of Ru/C and a test solution (120 mL) with desired background salt (NaCl, $NaHCO_3$, and/or Na_2SO_4) concentrations were added to a 250 mL three-neck flask equipped with rubber stoppers and a Teflon-coated magnetic stir bar (Fig. 2a). Initial rates were collected for the Ru/C loading ranging from 1 to 7.5 g L^{-1} to identify the conditions under which external mass transfer limitations are absent at the selected stirring speed (1100 rpm). Prior to initiating the reaction with nitrate, Ru/C in aqueous suspension was maintained under 1 atm H_2 headspace overnight by flowing excess H_2 gas through the reactor (300 mL min^{-1}) while continuously stirring. The pretreatment duration was chosen to accommodate reactor schedule, and a shorter duration will likely be acceptable and can be confirmed in future process optimization studies. Reaction was initiated by adding a small volume of concentrated $NaNO_3$ stock solution (5 M)

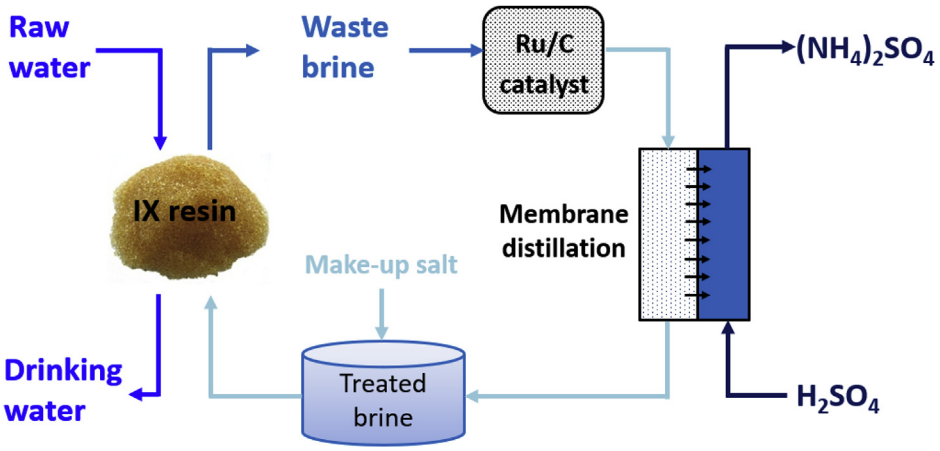

Fig. 1. Flow diagram of the proposed hybrid ion exchange/catalytic hydrogenation/membrane distillation (IX/CH/MD) strategy for reducing salt input requirements and waste brine discharge volumes while simultaneously recovering a nitrogen fertilizer product during treatment of nitrate-contaminated water sources.

Table 1
Waste ion exchange brine composition.

Component	Concentration (mg L^{-1})
pH	8.5
Total inorganic C	3057
Total organic C	22.5
HCO_3^-	13,100 as $CaCO_3$
Cl^-	13,700 (2.3 wt% as NaCl)
NO_3^-	9260 (149 mM)
NO_2^-	BQL[a]
SO_4^{2-}	4350 (45 mM)
PO_4^{3-}	BQL[a]
Na	16,900
K	35.7
Mg	15.8
Ca	5.8
Cr	2.9
V	1.2
Li	0.6
Mo	0.5
Sr	0.2

[a] BQL = below quantification limit (instrument quantification limit 0.1 mg L^{-1}, method quantification limit 10 mg L^{-1} at dilution factor of 100).

to achieve the designed initial nitrate concentration (50–200 mM), and reaction progress was tracked by periodically collecting aliquots of the catalyst suspension (1.5 mL) for analysis; collected aliquots were immediately filtered (0.45 μm cellulose acetate) to quench the reaction. Reaction temperature was maintained with a circulating external water bath calibrated by an external thermometer. The change of solution pH over the course of reaction was monitored (Orion double junction combination pH electrode, calibrated by standard NIST buffers, apparent pH values were reported). In the case where the effect of pH on reactions was evaluated, solution pH was maintained by an automatic pH-stat (Metrohm) using HCl. The collected filtrate aliquots were diluted with deionized water and analyzed for nitrate, nitrite, and/or ammonia concentrations. All experiments were performed in duplicate, and uncertainties are reported as standard deviations.

The procedure for measuring catalytic hydrogenation of nitrate in real waste brine was modified to avoid the complication of nitrate reduction occurring during the period where the catalyst was pre-exposed to H_2 gas overnight. Prior to the reaction, a small volume Ru/C slurry (0.6 g Ru/C in 10 mL deionized water) was reduced overnight under H_2 flow (300 mL min^{-1}) at room temperature. Reaction was then initiated by introducing 100 mL of the

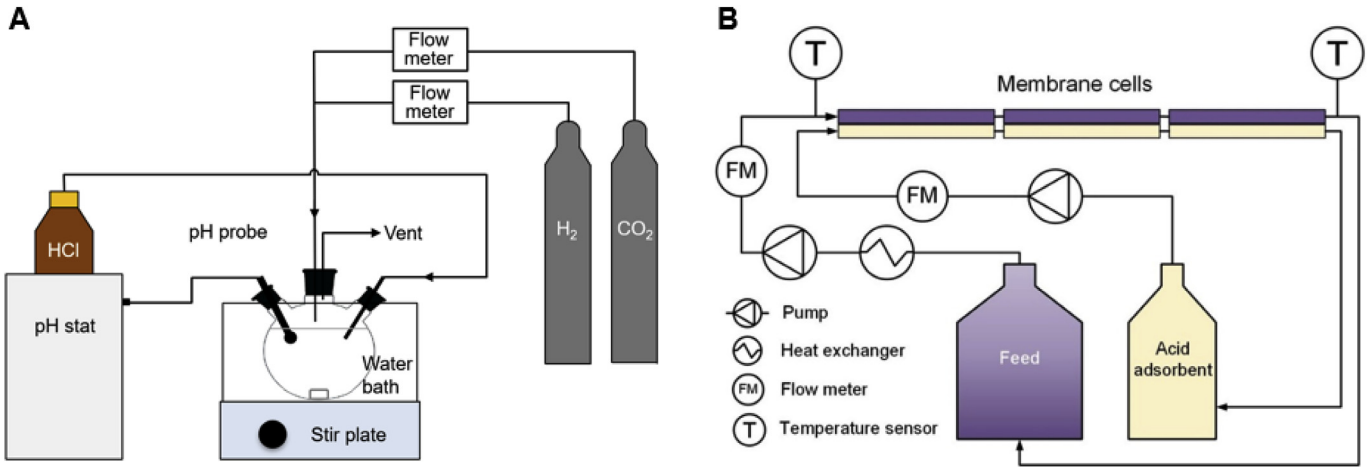

Fig. 2. Schematic diagram of the bench scale (a) catalytic hydrogenation reactor and (b) membrane distillation system.

waste brine to a flask containing the pre-reduced catalyst. As a control, experiments were also conducted in a synthetic brine prepared to mimic the major ion composition of the real waste brine (Table 1). For tests where $CO_{2(g)}$ was used to buffer pH of the brine during treatment, CO_2 gas was introduced to the reactor at 65 mL min^{-1}. The rest of the procedure follows the description provided above. A catalyst recycle experiment was also carried out to evaluate the reusability of Ru/C for waste brine treatment. At the end of the reaction, the catalyst was collected by filtering the suspension with a membrane filter (0.45 μm cellulose acetate), rinsed with deionized water several times, and dried in air at 70 °C before reusing in the next reaction cycle.

2.3. Membrane distillation experiments

A bench-scale membrane distillation assembly was operated in direct contact batch mode to recover ammonia from synthetic brine and real waste brine that was first catalytically treated to reduce nitrate to ammonia (Fig. 2b). Ammonia-containing brine solutions were on the feed side and sulfuric acid (0.25 M) was used on the absorbent side of the membrane assembly. The membrane cell was custom-made acrylic plastic cell, and spacers were used in both the feed and the acid absorbent channels of the cell. The cell was outfitted with a hydrophobic, microporous membrane provided by BHA Altair, LLC (QL822). The membrane is a polypropylene-backed PTFE material with a nominal pore size of 0.45 μm with the functional layer in contact with the feed. Three cells, each with a surface area of 195 cm^2, were used in series. The experiments were performed using co-current flow to minimize the local pressure differential across the membrane. The feed stream was pumped continuously during operation using a positive-displacement gear pump (Micropump Integral Series, IDEX Corp. Vancouver, WA). The acid absorbent stream was also pumped continuously using a peristaltic pump (Masterflex L/S Series, Cole-Parmer, USA). Flow rates of the feed and the acid absorbent were kept equal. A heat exchanger was used to control the temperature of the feed brine stream. Tests were conducted prior to ammonia recovery experiments to validate membrane integrity and ensure that the membranes were not wetted.

Four liters of brine feed solution was used for each experiment. The concentration of H_2SO_4 in the acid absorbent (0.25 M, 1–2 L) was designed to be excessive to ensure complete capture of ammonia passing through the membrane as $(NH_4)_2SO_4$. Kinetic studies were conducted with synthetic solutions to examine the impact of operating parameters on ammonia recovery. The synthetic solutions were prepared by dissolving predetermined amount of salts (NaCl, $NaHCO_3$, and/or Na_2SO_4), ammonia aqueous solution, and base (NaOH) in deionized water. The amount of ammonia in aqueous solutions and NaOH was determined by assuming complete hydrogenation of nitrate according to the following stoichiometry (Eq (1)):

$$NO_3^- + 4H_2 \rightarrow NH_3 + OH^- + 2H_2O \quad (1)$$

Time zero was recorded once the feed reached the designed temperature (heat-up time 1–2 min), and the test duration was 60 min. Feed solution was sampled (8–10 mL) periodically to track the change of total ammonia concentration (i.e., $[NH_4^+] + [NH_3]$). For selected tests, acid absorbent solution was also sampled (1 mL) to quantify the mass balance on ammonia in the system. The initial and final pH values of the feed were also recorded. Batch experiments were performed in duplicate and uncertainties are reported as standard deviations. The procedure for catalytically treated real waste brine was the same as for synthetic brine.

2.4. Aqueous analysis

Anions, including Cl^-, NO_3^-, SO_4^{2-}, NO_2^-, and PO_4^{3-}, were quantified by ion chromatography with conductivity detection (ICS-90, Dionex, Sunnyvale, CA). Metals were quantified by inductively coupled plasma–atomic emission spectroscopy (ICP-AES; Optima 5300, PerkinElmer, Fremont, CA). ICP-AES samples were acidified with nitric acid to a pH < 2 before analysis. Total ammonia (NH_3/NH_4^+) was analyzed by colorimetric analysis (Hach salicylate method). Alkalinity was measured by titration with 1 N H_2SO_4. Total organic carbon (TOC) and inorganic carbon were determined using a total organic carbon analyzer (Shimadzu TOC-L, Columbia, MD).

3. Results and discussion

3.1. Synthetic brine – catalytic nitrate hydrogenation

Catalytic hydrogenation with Ru/C was initially evaluated in synthetic brine solutions prepared at conditions representative of nitrate-contaminated waste IX brines, designed to assess the influence of major anions and operating conditions. Tests showed that the initial rate of nitrate hydrogenation increased linearly with the catalyst loading ranging from 1 to 7.5 g L^{-1} (Fig. S1), consistent with negligible external mass transfer limitations (Huo et al., 2017; Rao et al., 1998; Ruppert et al., 2009). However, the possibility of internal mass transfer limitations within the catalyst particles cannot be ruled out, which is an inherent challenge for porous catalyst materials (Choe et al., 2015). A catalyst loading of 5 g L^{-1} was then selected for use in subsequent experiments. Fig. 3 shows the time profile of nitrate hydrogenation observed under the baseline testing conditions (100 mM initial nitrate concentration + 5 g L^{-1} Ru/C in 5 wt% NaCl, 100 mM $NaHCO_3$, 100 mM Na_2SO_4, 30 °C, no pH control). The rate of nitrate hydrogenation appeared to be constant for the first half-life. Although this observation alone is not sufficient to formally establish reaction order, we calculated apparent zero-order rate constants using data collected for the first half-life to facilitate comparison of catalyst

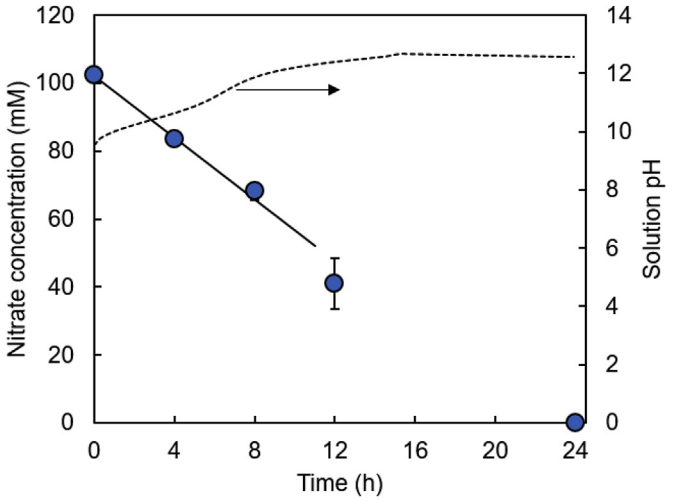

Fig. 3. Catalytic nitrate hydrogenation and evolution of solution pH under baseline testing conditions. Conditions: 5 g L^{-1} Ru/C, $[NO_3^-]_0$ = 100 mM, synthetic brine matrix (5 wt% NaCl, 100 mM $NaHCO_3$, 100 mM Na_2SO_4), 30 °C, no solution pH control, 1 atm H_2 headspace maintained by flowing H_2 at ca. 300 mL min^{-1}. Error bars indicate standard deviation from duplicate measurements (smaller than symbol if not visible). Solid line indicates zero-order rate law fit to the first half-life. Dashed line indicates change in measured pH during the reaction.

activity under different feed solution chemistries and operating conditions within the given system and also with catalyst activities reported in literature (Bergquist et al., 2016; Choe et al., 2015).

$$[NO_3^-] = [NO_3^-]_0 - k_0 M_{Ru} t \quad (2)$$

where $[NO_3^-]_o$ is the initial aqueous nitrate concentration (mM), $[NO_3^-]$ is the aqueous nitrate concentration at reaction time t (min), and k_0 is the apparent zero-order rate constant normalized to Ru metal mass in the reactor suspension (mM min^{-1} g_{Ru}^{-1}), and M_{Ru} is the mass loading of active Ru metal in the aqueous suspension (g_{Ru} L^{-1}). Under the baseline testing condition, k_0 was found to be 0.30 ± 0.03 mM min^{-1} g_{Ru}^{-1}. This value falls within the same order-of-magnitude as values reported for Pd–In/C catalysts using a similar semi-batch reactor (0.18–0.81 mM min^{-1} g_{Pd}^{-1}) (Choe et al., 2015), indicating comparable activity and feasibility for treating waste IX brine with Ru-based catalysts. This finding is also notable because market costs for Ru have historically been much lower than Pd (Chen et al., 2017; Huo et al., 2017; Vardon et al., 2017). Ammonia was the only product in the liquid phase, but nitrogen mass balance closure was hindered by NH_3 transfer to the flowing H_2 in the headspace. We confirmed the selective nitrate reduction to ammonia based on real IX waste brine treatment results as shown later.

The values of k_0 measured in synthetic brines of varying composition are summarized in Table 2. An inverse dependence was observed between k_0 and initial nitrate concentration. Reducing the initial nitrate concentration from 100 mM to 50 mM resulted in k_0 increasing from 0.30 to 0.70 mM min^{-1} g_{Ru}^{-1}, while increasing the initial nitrate concentration to 200 mM resulted in k_0 decreasing to 0.08 mM min^{-1} g_{Ru}^{-1}. This trend suggests that the zero-order behavior observed for individual batch reactions may not represent the inherent nitrate hydrogenation kinetics. Considering the potential influence of products on reaction rates, a more formal approach to study kinetics in batch reactor is to examine the relationship between initial rate and initial concentrations (Ngo et al., 2018; Tadepalli et al., 2007).

$$-\frac{d[NO_3^-]_0}{dt} = k[NO_3^-]_0^a [H_2]_0^b \quad (3)$$

$$\ln\left(-\frac{d[NO_3^-]_0}{dt}\right) = a \ln[NO_3^-]_0 + b\ln[H_2]_0 + \ln k \quad (4)$$

where k is the rate constant, a and b are the reaction orders for nitrate and hydrogen, respectively, and $[H_2]_o$ is the initial aqueous concentration of hydrogen, which is proportional to hydrogen partial pressure in the gas phase according to Henry's law. Because k and $[H_2]_o$ are constant in the current system, a can be obtained from the slope of plotting the natural log of initial nitrate hydrogenation rate versus the natural log of initial nitrate concentration. A value of −1.5 was obtained for a over the range of nitrate concentration tested in this study (Fig. S2), which indicates the saturation of the catalyst surface with nitrate and therefore blocking H_2 adsorption (Nijhuis et al., 2002). The non-integer is challenging to be completely rationalized, and further study of initial rates with well-controlled system free of non-target ions (e.g., NaCl) is needed to develop a more formal kinetic model for catalytic nitrate reduction in brine solutions.

Because the nitrate hydrogenation reaction generates OH^- as a product (Eq. (1)), solution pH increases as nitrate hydrogenation proceeds in the absence of an appropriate buffer. Under the baseline condition, solution pH increased from an initial value of 9.5 to a final value of 12.6 by the end of the reaction (Fig. 3). To evaluate the potential influence of solution pH on nitrate hydrogenation, apparent zero-order rate constants were determined for reactions where pH was maintained at circumneutral pH conditions (pH 7.5) and basic pH conditions (pH 11) by automatic pH-stat (with HCl addition). Similar reaction rate constants were observed at both pH conditions (Table 2), with k_0 only increasing by ~20% at the higher pH conditions. At first glance, the limited effect of changing solution pH appears to contradict findings reported previously for the same catalyst reacting with lower initial nitrate concentrations (e.g., 1.6 mM instead of 100 mM), where the first-order reaction constant decreased at basic conditions (Huo et al., 2017). However, the differing pH-dependent trends can be attributed to how pH affects the concentration of nitrate adsorbing to catalyst surfaces at different nitrate concentrations. With increasing pH, the catalyst surfaces become more negatively charged due to deprotonation of acidic surface functional groups on the support and accumulation of OH^- on the metal surface (Abdelrahman et al., 2015), inhibiting electrostatic attraction and decreasing affinity for adsorption of oxyanions like nitrate. At lower nitrate concentrations in the solution phase this can inhibit reaction of nitrate with adsorbed

Table 2
Summary of measured initial rate constants for nitrate hydrogenation in synthetic brines (1 atm H_2, 5 g L^{-1} Ru/C).

NaCl wt%	$NaHCO_3$[a] mM	Na_2SO_4 mM	$NaNO_3$[a] mM	Temp °C	pH	k_0 mM min^{-1} g_{Ru}^{-1}
Baseline condition						
5	100	100	100	30	No control, rising pH	0.30 ± 0.03
Varying initial nitrate concentration						
5	100	100	50	30	No control, rising pH	0.70 ± 0.07
5	100	100	200	30	No control, rising pH	0.08 ± 0.01
Varying solution pH						
0	0	0	100	30	7.5	0.09 ± 0.01
0	0	0	100	30	11	0.11 ± 0.01
Varying salt levels						
0	0	0	100	30	No control, rising pH	0.15 ± 0.01
5	0	100	100	30	No control, rising pH	0.16 ± 0.03
0	100	0	100	30	No control, rising pH	0.58 ± 0.01
10	100	200	100	30	No control, rising pH	0.10 ± 0.01
Varying temperature						
5	100	100	100	25	No control, rising pH	0.18 ± 0.01
5	100	100	100	35	No control, rising pH	0.32 ± 0.04

[a] Amounts.initially added.

atomic hydrogen by decreasing the pre-equilibrium concentrations of adsorbed nitrate (Chen et al., 2010; Epron et al., 2002; Wang et al., 2014). While the intrinsic affinity of nitrate for adsorption to the surface is still likely reduced when higher initial nitrate concentrations are used, the very high concentration of nitrate in the solution (100 mM) is still sufficient to drive the nitrate adsorption to achieve high nitrate surface coverage. As a result, the apparent rate of nitrate hydrogenation is little affected by the change in solution pH conditions.

Three major non-target anions in waste brines and reused brines (i.e., chloride, bicarbonate, and sulfate, Table 1) were then systematically evaluated for their influence on nitrate hydrogenation activity with Ru/C. Removal of all three anions from the solution led to a 50% decrease in k_0 (from 0.30 to 0.15 mM min^{-1} g_{Ru}^{-1}, Table 2). Similar reductions in k_0 were found in the pH-buffered experiments mentioned above where the three ions had also been removed from the matrix. Collectively, these observations indicate that either increases in overall salinity of the water promotes catalyst reactivity with nitrate or that more specific interaction involving one or more of the major anions acts to promote nitrate reactions. Subsequent experiments suggest that the bicarbonate anion component is particularly important to catalytic reactions with nitrate. The rate constant measured in brine prepared without the bicarbonate component (0.16 mM min^{-1} g_{Ru}^{-1}) was similar to the value measured in the absence of all three major anions (0.15 mM min^{-1} g_{Ru}^{-1}), whereas the rate constant measured in solution containing only the bicarbonate component (0.58 mM min^{-1} g_{Ru}^{-1}) was nearly four times the value measured with no brine components and twice the value measured in the baseline brine condition where all three major anions were present. On the other hand, doubling the chloride and sulfate components decreased k_0 (from 0.30 to 0.10 mM min^{-1} g_{Ru}^{-1}). Collectively, these findings indicate that chloride and sulfate anions competitively inhibit nitrate reactions with Ru/C, but bicarbonate anions serve to promote increased catalytic reactions of nitrate. The inhibitory effects of chloride and sulfate are consistent with observations reported for Pd-based catalysts (Bergquist et al., 2016; Choe et al., 2015; Pintar et al., 1998), which are attributed to competitive inhibition of nitrate adsorption. The reason for enhanced reactivity in the presence of elevated concentrations of bicarbonate is less clear. This ion differs from the other two in that it possesses a labile proton:

$$HCO_3^- \leftrightarrow H^+ + CO_3^{2-} \quad pK_a = 10.33 \tag{5}$$

Nitrate reduction to ammonia consumes H^+ (Eq. (1)), so it is possible that bicarbonate can serve as a proton donor in the rate-determining step on the overall reaction, thereby increasing the apparent rate of nitrate hydrogenation.

Lastly, increasing solution temperature from 25 to 35 °C showed a positive effect on k_0 (Table 2), similar to reports of nitrate reduction with Pd-based catalysts (Kim et al., 2016; Soares et al., 2012). Arrhenius plot of the data yielded an apparent activation energy (E_a) of 45 ± 6 kJ mol^{-1}, comparable to E_a reported for nitrate hydrogenation with a Pd−Cu/Al_2O_3 catalyst (Pintar et al., 1996). In sum, the nitrate hydrogenation experiments conducted in synthetic brine solutions support the technical feasibility of applying Ru/C catalyst for reduction of nitrate ions present in IX waste brines. The effects of different constituents and operating conditions on reaction kinetics will inform future process design efforts. For example, waste heat sources, if present, may be leveraged to improve reaction rates, which can also benefit subsequent recovery of ammonia by membrane distillation, as discussed below.

3.2. Synthetic brine - ammonia recovery by membrane distillation

Catalytic nitrate hydrogenation with Ru/C generates an ammonia-rich brine. The ammonia is then removed from the brine by membrane distillation and recovered as $(NH_4)_2SO_4$ in a H_2SO_4 trap solution (Fig. 2b). A similar approach to that used for catalytic hydrogenation studies was employed to evaluate ammonia recovery from synthetic waste IX brines by membrane distillation and identify the effects of important operating factors. Under the baseline testing conditions, a synthetic brine feed was designed to have the same composition as the baseline testing solution for catalytic hydrogenation, with the exception that nitrate is assumed to be hydrogenated stoichiometrically to ammonia according to Eq. (1). Solution conditions, including salt levels, solution pH, initial ammonia concentration, and temperature were evaluated for their impact on ammonia recovery efficiency. Initial testing was used to select 1.5 L min^{-1} feed flow rate to allow for good mixing conditions at the boundary layer (Qu et al., 2013) while maintaining the system at low pressure (7.5 psig) to reduce the risk of wetting the membranes (Qi and Cussler, 1985).

Under the baseline conditions, the kinetics of ammonia removal from the feed followed a first-order rate law over the entire reaction time course (Fig. 4). Nitrogen mass balance closure was achieved when summing the total ammonia concentrations in the feed and acid absorbent sides of the membrane, indicating that the system was well sealed, and loss of ammonia to void spaces in the system was negligible. The membranes employed in membrane distillation process are hydrophobic, allowing vapor-phase species to permeate while rejecting ionic constituents in the aqueous feed. Also, because the temperatures of the feed and absorbent solutions were the same in the baseline testing conditions, the driving force for ammonia mass transfer was only the difference in ammonia partial vapor pressure between the feed and the acid absorbent. The latter was maintained at a minimum by trapping the absorbed ammonia in the protonated ammonium state that predominates in acidic solutions.

$$NH_4^+ \leftrightarrow H^+ + NH_3 \quad pK_a = 9.25 \tag{6}$$

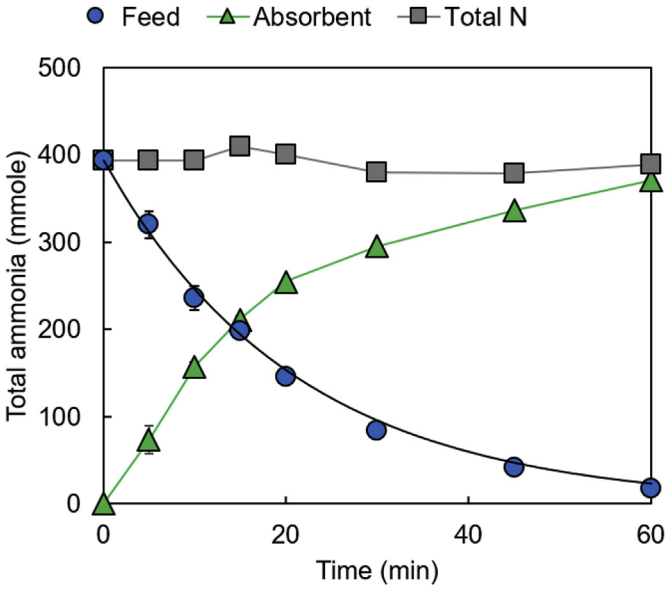

Fig. 4. Ammonia removal from synthetic brine by membrane distillation and mass balance under baseline testing conditions. Black solid line for Feed represents the first-order model fit, whereas lines for Absorbent and Total N are only added to aid the eye.

Table 3
Summary of ammonia mass transfer coefficient (K_{MD}) and initial mass flux (J_{NHa}) with different feed characteristics and operating conditions.

NaCl wt%	$NaHCO_3$[a] mM	Na_2SO_4 mM	Ammonia[a,b] mM	Temp °C	Initial pH	Final pH[c]	K_{MD}[b] m h^{-1}	Initial J_{NH3}[b] gNH_3-N m^{-2} h^{-1}
Baseline condition								
5	100	100	100	30	11.2	10.8	0.19 ± 0.01	268 ± 3
Varying salt levels								
0	100	0	100	30	11.6	11.3	0.19 ± 0.02	258 ± 21
10	100	200	100	30	11.1	10.7	0.18 ± 0.02	258 ± 26
Varying solution pH and initial ammonia concentration								
5	50	100	50	30	11.1	10.7	0.20 ± 0.03	141 ± 21
5	200	100	50	30	9.2	9.1	0.10 ± 0.01	71 ± 1
5	50	100	200	30	12.7	12.6	0.16 ± 0.02	457 ± 49
5	200	100	200	30	11.5	11.0	0.17 ± 0.01	482 ± 39
Varying temperature								
5	100	100	100	25	11.2	10.9	0.16 ± 0.01	229 ± 3
5	100	100	100	35	11.2	10.7	0.23 ± 0.03	326 ± 37

[b]Operation time 1 h.
[a] Amounts initially added.
[b] Calculated by using total ammonia concentration (i.e., $[NH_4^+] + [NH_3]$).

The feed solution pH decreased from 11.2 to 10.8 as the ammonia was removed, consistent with removal of a base species from solution (Tao and Ukwuani, 2015). With very few exceptions, feed solution pH remained >10.7 during the tests, where free ammonia species predominates (>96%) (Table 3). Due to the relatively low temperatures studied (no higher than 35 °C for all tests), water evaporation through the membranes was not expected to be significant. Therefore, the mass flux of ammonia (J_{NH3}; gNH_3-N m^{-2} h^{-1}) from the feed to the acid absorbent can be represented by the following equation:

$$J_{NH3} = K_{MD}[NH_3]_f \quad (7)$$

where K_{MD} is the overall mass transfer coefficient (m h^{-1}), and $[NH_3]_f$ is the concentration of free ammonia in the feed solution ($mgNH_3$-N L^{-1}). The overall mass transfer coefficient comprises three resistances (i.e., feed liquid side boundary resistance, membrane resistance, and acid absorbent side boundary resistance) and depends on the membrane and operating conditions (Zarebska et al., 2014). Practically, the value of K_{MD} can be determined by the following equation (du Preez et al., 2005; El-Bourawi et al., 2007; Zarebska et al., 2014):

$$K_{MD} = \frac{V}{At}\ln\left(\frac{[NH_3]_{f,0}}{[NH_3]_f}\right) \quad (8)$$

where V is the total volume of the feed (m^3), A is the membrane area (m^2), $[NH_3]_{f,0}$ is the initial concentration of ammonia in the feed (mM), and $[NH_3]_f$ is the ammonia concentration in the feed at time t (h). By plotting $\ln([NH_3]_{f,0}/[NH_3]_f)$ versus time, a straight line with the slope of $(K_{MD}\cdot A)/V$ was obtained, and subsequently K_{MD} was determined. The initial J_{NH3} was then calculated from Eq. (7). Under the baseline condition, the initial J_{NH3} was found to be 268 gNH_3-N m^{-2} h^{-1} with the corresponding K_{MD} of 0.19 m h^{-1} (Table 3).

Direct comparison of kinetic parameters observed in this study with those reported in the literature is challenging, because rates of ammonia mass transfer strongly depend on several factors, including system configuration and geometry, membrane properties, and hydrodynamic characteristics of the system (Arogo et al., 1999; Bennett and Myers, 1983; Lauterböck et al., 2013; Qi and Cussler, 1985). Consequently, ammonia mass transfer coefficients using model ammonia aqueous solution by membrane contactors vary over a few orders-of-magnitude, e.g., 10^{-5} m s^{-1} (10^{-4} m h^{-1}) (Ding et al., 2006; Zhu et al., 2005), 10^{-3} m h^{-1} (Ahn et al., 2011), and 0.62 cm s^{-1} (0.37 m h^{-1}) (Qi and Cussler, 1985). The K_{MD} values measured in this study fall on the higher end of values reported. Even so, ammonia recovery under different feed solution chemistry and operating conditions can be compared within the given system.

Variable salt concentration and composition in the brine feed solutions (0–10 wt% for NaCl, 0–200 mM for Na_2SO_4) had only a minor effect on ammonia mass transfer (Table 3). Increasing ionic strength has slightly negative effect on the fraction of free ammonia species present at a given pH condition (Bower and Bidwell, 1978). However, at the relatively high pH conditions (>10.7, 1.45 pH units above the pK_a) used in these tests, the fraction of free ammonia species remained high, rendering the effect of ionic strength insignificant.

During catalytic nitrate hydrogenation, solution pH and free ammonia concentration were inherently coupled due to the hydroxide generated during the reaction (Eq. (1)). In addition, pH of the brine solution was influenced by the buffering capacity of the solution during catalytic hydrogenation. Accordingly, four test conditions were designed that combined two factors relevant to solution pH, i.e., ammonia concentration, and bicarbonate concentration, each at two levels. To simplify the synthetic solution preparation, we added pre-determined amounts of ammonia, bicarbonate and hydroxide following reaction stoichiometry (Eq. (1)) assuming complete nitrate hydrogenation without loss of ammonia to the gas phase. At relatively low buffering capacity (e.g., 50 mM initial ammonia and 50 mM initial bicarbonate), feed solution pH was >11, and measured K_{MD} (0.20 m h^{-1}) was similar to that observed for the baseline testing condition (Table 3). On the other hand, when the brine was initially more strongly buffered at circumneutral pH conditions (e.g., 50 mM initial ammonia and 200 mM initial bicarbonate), feed solution for membrane distillation had a lower initial pH value. With an apparent solution pH of 9.2, a condition wherein only ~50% of the ammonia is present as the free ammonia species and ~50% as NH_4^+, the measured value of K_{MD} (calculated based upon total ammonia concentration) decreased 51% (Table 3), suggesting that feed solution pH can strongly influence rates of ammonia mass transfer. For brines with higher initial ammonia concentration (e.g., 200 mM), solution pH was generally higher (>11), and measured K_{MD} values were again comparable with that observed for the baseline testing condition (Table 3). The initial J_{NH3} was observed to increase with the initial ammonia concentration, which was expected from Eq. (8).

As expected, increasing temperature of the feed solution also had a positive effect on ammonia mass transfer. For example, K_{MD} decreased from the baseline condition (30 °C) to 0.16 m h^{-1} when

temperature was reduced to 25 °C, and increased to 0.23 m h^{-1} when temperature was increased to 35 °C (Table 3). This influence of temperature observed was consistent with literature findings with various membrane distillation configurations, including vacuum and sweep gas membrane distillation (Ding et al., 2006; Wu et al., 2016; Xie et al., 2009). With increasing feed solution temperature, solute diffusivity increases, ammonia solubility decreases, and dissociation equilibrium is disturbed to favor dissociation, which all can contribute to higher mass transfer rates (Arogo et al., 1999). However, increasing feed temperature to accelerate ammonia mass transfer will be increasingly limited at higher temperatures, because the mass transfer of water vapor through the membrane is intensified, compromising ammonia selectivity (Xie et al., 2009).

Although membrane distillation has previously been explored for ammonia removal from wastewater, its application in a concentrated brine matrix such as waste IX brine was evaluated for the first time in this study. The relatively high K_{MD} values reported here indicate that the chosen membrane has desirable properties for such applications and the system geometry and liquid flow rate imparted thin liquid boundary layer to minimize mass transfer resistance. Similar to previous studies, high feed solution pH and temperature were identified as critical variable for ammonia mass transfer. Further sensitivity analysis will be useful to optimize process operation by determining the relative changes of ammonia mass transfer coefficient per "unit" change of operating factor (Arogo et al., 1999).

3.3. *Demonstration of nitrate removal and ammonia recovery from real waste brine*

Based on the results obtained in synthetic brines, we conducted a demonstration of nitrate reduction and ammonia recovery with a real ion exchange waste brine obtained from a utility in California

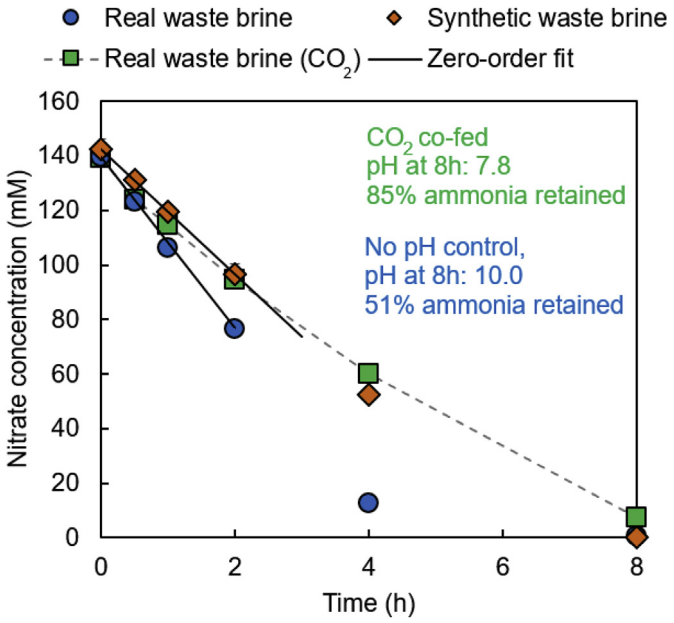

Fig. 5. Catalytic nitrate hydrogenation in real waste brine and a synthetic "mimic" waste brine prepared with similar anionic composition as the waste brine. Conditions: 6 g L^{-1} Ru/C, 30 °C, no solution pH control, 1 atm H_2 headspace maintained by flowing H_2 at ca. 300 mL min^{-1}. The effect of pH control by flowing CO_2 (at ca. 65 mL min^{-1}) was also examined. Error bars indicate standard deviation from duplicate measurements (smaller than symbol if not visible). Solid lines indicate the zero-order model fits to the first half-life.

treating nitrate-contaminated groundwater (Table 1). Catalytic nitrate hydrogenation in the waste brine followed a zero-order rate law (Fig. 5), similar to synthetic brine solutions. However, the measured k_0 value was found to be significantly higher (1.80 ± 0.04 mM min^{-1} g_{Ru}^{-1}) than the values measured in the synthetic brines (Table 2). As a control, reaction was conducted in a synthetic waste brine with the same concentrations of major anions (chloride, nitrate and sulfate), alkalinity (by adding sodium bicarbonate), and initial solution pH (adjusted with NaOH) as the real waste brine. Interestingly, the k_0 value measured in this synthetic "mimic" waste brine was ~30% lower (1.24 ± 0.02 mM min^{-1} g_{Ru}^{-1}) than the value measured in the real waste brine. These results verify the technical feasibility of applying Ru/C for nitrate hydrogenation in ion exchange waste brine. Still, further research is needed to identify the origin of the faster nitrate hydrogenation kinetics observed in the real waste brine. It is noted that the real waste brine contains multiple minor constituents that are absent in the synthetic waste brine. For example, the sole cation used in the preparation of synthetic waste brine is Na^+, while the real waste brine contains several divalent and trivalent cations (e.g., Ca^{2+}, Mg^{2+}), which have previously been shown to enhance rates of nitrate hydrogenation (Pintar et al., 1998). In addition, trace organics and metals in the real waste brine may interact with catalyst surfaces to enhance nitrate reactivity (Hörold et al., 1993; Liu et al., 2014; Moyer and Meyer, 1979).

Considering that bicarbonate showed positive influence on nitrate hydrogenation kinetics (Table 2), tests were conducted to co-feed CO_2 with H_2, which is a common practice for pH control when treating nitrate with Pd-based catalysts (Bergquist et al., 2016; Choe et al., 2015). The nitrate hydrogenation rate was comparable with that in the absence of CO_2 for the first 0.5 h, but the rate gradually decreased with further reaction time (Fig. 5). This observation could be a result of lower hydrogen partial pressure and the accumulation of anionic bicarbonate and carbonate over time to compete with nitrate for active site adsorption. For example, the inorganic carbon concentration increased from 238 mM to 466 mM after 12 h of treatment. On the other hand, co-feeding CO_2 significantly improved retention of ammonia in the open reactor system by maintaining solution pH between 7.6 and 7.9, where ionic NH_4^+ predominates over the free ammonia species. After 8 h of reaction, 85% of the ammonia was retained in the liquid phase when co-feeding CO_2 compared to only 51% in the absence of CO_2 buffer, where pH increased to 10.0, allowing conversion of NH_4^+ to the volatile NH_3 species (Fig. S3).

To provide sufficient feed solution for the membrane distillation experiments, catalytic hydrogenation of real waste brine was scaled up in 1 L reactors (from 0.25 L flasks in experiments discussed to this point). Reaction was conducted for up to 24 h while co-feeding CO_2 to maximize ammonia retention in the liquid phase. These conditions resulted in near complete nitrate hydrogenation, and the liquid phase retained ~90% of the ammonia reaction product (Table 4). Salt composition analysis showed no loss of chloride and sulfate, while inorganic carbon concentration increased due to CO_2 absorption (Table 4). Further reactor optimization can be used to improve reaction kinetics, but this is beyond the scope of the present proof-of-concept study. Following catalytic reaction and just prior to beginning the membrane distillation experiment, the solution pH was adjusted to ~10.0 with NaOH to better reflect the pH conditions observed when pH was allowed to drift without CO_2 buffer.

Fig. 6a shows the observed kinetics of ammonia removal from the catalytically treated real waste brine and a synthetic brine prepared with the same major ion composition, total ammonia, and pH as the treated real waste brine. Ammonia removal in both brine matrices were similar and followed a first-order model. Model fit of

Table 4
Water quality comparison of the real waste brine before treatment, after catalytic hydrogenation with Ru/C, and after membrane distillation to recover ammonia.

Solution chemistry	Real waste brine	After hydrogenation	After membrane distillation
pH	8.5	8.6	9.9[a]
Cl^-	13,700 mg L^{-1} (2.3 wt% as NaCl)	14,200 mg L^{-1} (2.4 wt% as NaCl)	14,200 mg L^{-1} (2.4 wt% as NaCl)
HCO_3^-/CO_3^{2-}	232 mM	485 mM	484 mM
NO_3^-	9260 mg L^{-1} (149 mM)	79 mg L^{-1} (1.2 mM)	75 mg L^{-1} (1.2 mM)
SO_4^{2-}	4350 mg L^{-1} (45 mM)	4520 mg L^{-1} (47 mM)	4280 mg L^{-1} (45 mM)
Total ammonia	<3.2 mM[b]	136 mM	9 mM

[a] Solution pH was adjusted to 10.0 by adding NaOH prior to membrane distillation.
[b] Detection limit.

data collected in real waste brine yielded K_{MD} and J_{NH3} values of 0.11 m h^{-1} and 199 gNH_3-N m^{-2} h^{-1}, respectively (limited supplies of the catalytically treated waste brine prevented replicate experiments). This is similar to values measured in the synthetic brine ($K_{MD} = 0.12 \pm 0.01$ m h^{-1} and $J_{NH3} = 225 \pm 4$ gNH_3-N m^{-2} h^{-1}), and the K_{MD} value was of the same order of values obtained with other synthetic solutions (Table 3). Good nitrogen mass balance closure was also observed by summing the total ammonia concentrations in the waste brine feed and acid absorbent solutions (Fig. 6b). Salt composition and concentrations after membrane distillation were almost invariant (Table 4), verifying membrane integrity within tested operation time and high selectivity for transfer of ammonia. These results indicate that membrane distillation can be an effective process for recovering ammonia from real waste brine matrices.

Overall, the hybrid catalytic hydrogenation/membrane distillation process resulted in ~99% removal of nitrate from the waste brine and ~80% nitrogen recovery in form of aqueous $(NH_4)_2SO_4$. Small quantities of nitrogen (~7%) remained in the treated brine as either ammonia or nitrate, and the remainder was presumed to be lost to the gas phase during semi-batch catalytic reactions. While further improvements in system efficiency are likely through reactor optimization, findings reported here provide a proof-of-concept demonstration that the hybrid process can simultaneously treat nitrate contaminated waste brines and recover nitrogen as commercially viable fertilizer product.

3.4. Application considerations of the hybrid process

Compared with conventional brine treatment systems, the hybrid catalytic hydrogenation/membrane distillation process enables brine reuse and provides potentially valuable product through nitrogen transformation and recovery. Nitrogen in the form of dilute nitrate contamination present in the source water was transformed to a much more concentrated and pure $(NH_4)_2SO_4$ solution (Fig. 1), which can be used as a liquid fertilizer or a precursor for production of solid fertilizer (Amaral et al., 2016; Garcia-González and Vanotti, 2015; Li et al., 2018). This process leverages chemical potential difference as the driving force (e.g., nitrate adsorption to ion exchange resin, nitrate hydrogenation on Ru surface, and ammonia mass transfer across membrane) and has minimal thermal energy requirement; therefore, it likely has higher energy efficiency compared to the traditional high-energy Haber–Bosch ammonia synthesis from $N_{2(g)}$. The revenue from selling the $(NH_4)_2SO_4$ product may be approximated from the quantity and market price of $(NH_4)_2SO_4$. As an example, a medium-size water treatment plant (10 MGD) that removes 30 $mgNO_3$-N/L recovers 415 tonne NH_3–N/year, yielding 1960 tonne $(NH_4)_2SO_4$/year, which equates an annual revenue of $284,000 with an $(NH_4)_2SO_4$ price at $145/tonne (World Sulphuric Acid Weekly, 2017). Although producing $(NH_4)_2SO_4$ through the hybrid catalytic hydrogenation/membrane distillation process requires capital investment and consumption of H_2 and sulfuric acid, this process also reduces the costs for IX treatment by improving salt use

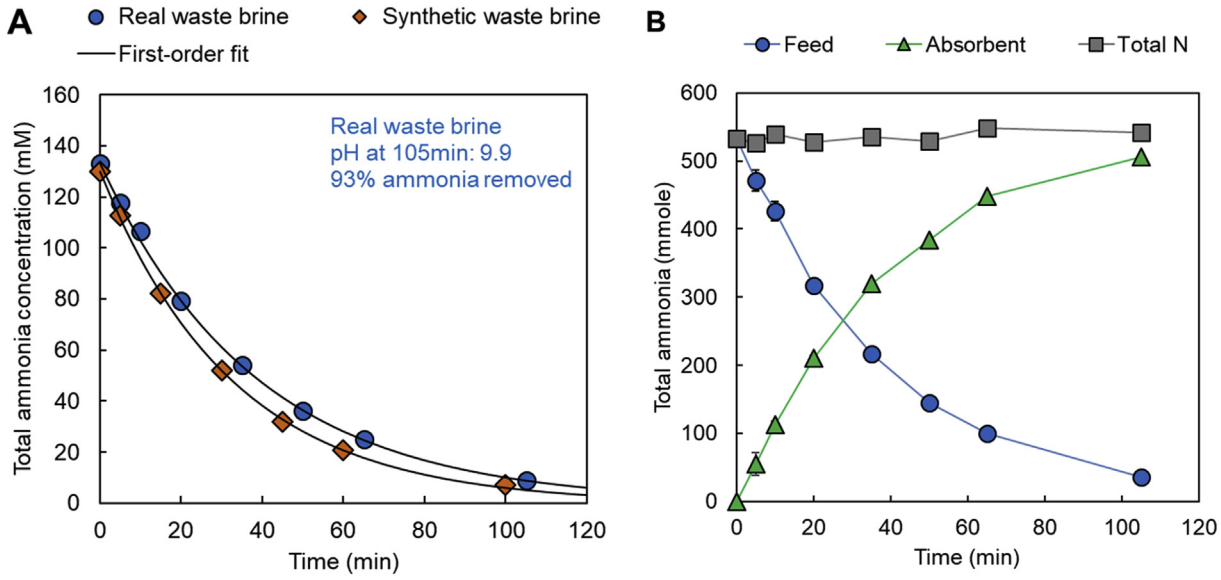

Fig. 6. (A) Ammonia removal from real waste brine and synthetic solution by membrane distillation. Conditions: 4 L feed flowing at 1.5 L min^{-1}, 1.15 L 0.25 M H_2SO_4 absorbent solution flowing at 1.5 L min^{-1}, 30 °C. (B) Ammonia mass balance in real waste brine feed and H_2SO_4 absorbent solution. Solid lines in (A) indicate the first-order model fits.

efficiency and drastically reducing waste brine disposal costs, while also limiting downstream environmental releases of nitrate (Wang et al., 2011). Therefore, a full techno-economic analysis and life cycle environmental impact assessment of the overall process are required to more rigorously evaluate the economics and environmental sustainability of the hybrid process demonstrated here. This analysis should include important factors, such as process scale and potential reductions in overall salt usage and waste discharge costs.

An initial conceptual evaluation of the economic and environmental viability of the catalytic hydrogenation process may be achieved by comparing the current system with a more developed brine treatment system using Pd-based catalysts (Bergquist et al., 2016; Choe et al., 2015). Previous work showed that both the O&M costs and environmental impacts of recycling IX brines by treating nitrate with Pd−In/C catalysts can be lower than those of conventional IX processes (Choe et al., 2015). A critical factor to delivering these benefits is reducing the catalyst cost, particularly the use of Pd (Chiueh et al., 2011). Catalyst cost is directly associated with the cost of the active metal (dominated by Pd for Pd−In/C catalysts) and catalyst quantity, which is determined by catalyst activity (less catalyst material is required for catalysts that exhibit higher activity). Along this line of consideration, Ru catalysts have an advantage over Pd-based catalysts due to the historically lower cost of Ru (Chen et al., 2017; Huo et al., 2017; Vardon et al., 2017). In addition, Ru catalysts have been reported to have high activity for nitrate reduction, similar to Pd−Cu/C catalysts (Huo et al., 2017). This study further confirmed that Ru/C is active for nitrate hydrogenation in various brine conditions. Although comparison between Ru/C activity determined in this study and that of Pd−In/C catalysts in the literature is not straightforward under different reaction conditions, their apparent zero-order rate constants normalized to metal mass are of similar magnitude when treating synthetic brine solutions, and the rate constant with Ru/C for treating a real waste brine is approximately two-fold higher than the highest value reported for Pd−In/C catalysts (Bergquist et al., 2016; Choe et al., 2015), all suggesting that Ru catalysts have a potential to improve the economic and environmental sustainability of the catalytic treatment step of the hybrid process.

A less studied but critically important consideration for catalytic processes is catalyst stability and longevity. Catalyst longevity is ultimately required to fulfill the assumptions of catalyst lifetime (usually years) during techno-economic analysis and life cycle assessment (Choe et al. 2013, 2015; Hutchison et al., 2017). Catalyst stability also affects catalyst loading design for a fixed volume of waste brine and vice versa, brine regeneration cycle design with a fixed loading of catalyst. Generally, the higher the total volume of waste brine that can be treated with the catalyst, the more savings that can be gained from brine reuse (Bergquist et al., 2016).

Ru/C stability for waste brine hydrogenation was initially assessed using a batch recycle test. After the first use, catalyst activity increased in the following cycles (Fig. S4). This increase in activity is likely related to catalyst activation. As shown in a previous study, elevated temperature pretreatment of catalysts with either inert (N_2) or reducing (H_2) gas environment improved the activity of Ru/C by desorbing synthesis residue and exposing redox-labile Ru species (Huo et al., 2017). ICP analysis of the filtrate from catalyst suspension after the reaction detected trace amounts of Ru (<0.2% of the total amount of Ru). However, it is unclear whether the detected Ru resulted from metal dissolution or the release of loosely bound Ru nanoparticles from attrition. These results demonstrated that Ru/C can be recycled in a semi-batch reactor, and catalyst deactivation through leaching or fouling is insignificant over four use cycles. Further study, ideally in packed-bed continuous-flow reactors, is required to more thoroughly determine the longer-term stability of Ru/C as well as process consumables and wastes during brine treatment and resource recovery applications. The time-on-stream performance of catalytic hydrogenation in flow reactors (Bergquist et al., 2017b; Chaplin et al., 2009; Mendow et al., 2011), including measures of nitrate hydrogenation activity, ammonia selectivity, and catalyst deactivation rates, will also be valuable for techno-economic analysis to optimize process design and identify critical cost drivers to guide further process development and optimization efforts. It has been reported that hydrogenation metal catalysts strongly adsorb sulfide species (Angeles-Wedler et al., 2008; Chaplin et al., 2006), which would lead to rapid catalyst poisoning if it were occurring in the system. Therefore, prevention of biological sulfate reduction in the brine recycling system will be critical to sustained operation.

Membrane distillation (or membrane contactor) has been considered a cost-effective, energy-efficient technology for removing ammonia from industrial and agricultural wastewater (Darestani et al., 2017; Xie et al., 2009). This study provided the first demonstration of its successful application to recovering ammonia from IX waste brine. The high ammonia removal efficiency observed in this study is related to the large membrane surface area, high feed flow rate, and prevailing high solution pH. As nitrate hydrogenation naturally raises solution pH (Eq. (1)), the membrane distillation process can benefit from an upstream catalytic reactor operated without pH control, which also saves the cost on alkali for adjusting pH for membrane distillation. Alternative membrane distillation configuration should be assessed to further improve unit efficiency and reduce membrane cost (Qu et al., 2013). A major concern during membrane distillation implementation is membrane fouling, such as by particulate and organics (Tijing et al., 2015; Warsinger et al., 2015; Zarebska et al., 2014). The risk of particulate fouling caused by catalyst particle can be reduced by filtration, which is also an effective method for removing scalants that might precipitate at higher solution pH conditions (e.g., calcium carbonate). On the acid absorbent side of the membrane, no solid precipitation is expected due to the high water solubility of $(NH_4)_2SO_4$. Organic fouling is of less concern for the ion exchange waste brine considering its low organic carbon content (Table 1), but the accumulation of organic carbon over several brine regenerant cycles may lead to fouling over long-term operation and needs to be evaluated. Further studies of membrane fouling during long-term operation of the hybrid treatment system is recommended.

4. Conclusions

This work demonstrated a hybrid catalytic hydrogenation/membrane distillation process that potentially enables ion exchange waste brine reuse and captures nitrogen in the form of fertilizer product. A commercial Ru/C catalyst, much lower in cost than widely studied Pd-based catalysts, was found to be active and selectively reducing nitrate to ammonia in both synthetic and real waste brine matrices. The resulting ammonia product was efficiently recovered from the brine by membrane distillation as aqueous $(NH_4)_2SO_4$, a commercial fertilizer product. Increased pH and temperature conditions in the feed solution increased rates of ammonia mass transfer through the gas permeable membrane, while salt composition and concentrations in the brine had little effect. The catalytic nitrate hydrogenation reaction naturally increases pH of treated brine, thereby facilitating ammonia recovery in the subsequent membrane distillation step. Low-grade waste heat sources, if available, can also be leveraged to enhance rates of both catalytic hydrogenation and membrane distillation steps. Demonstration of the hybrid process with a real ion exchange waste brine showed higher nitrate hydrogenation rates and similar rates of ammonia recovery compared to synthetic waste brines. The

higher rates of catalytic nitrate hydrogenation observed in the real waste brine suggests that trace brine components not reflected in the major ion composition can act to enhance reaction rates. Further studies are recommended to evaluate these factors specifically, assess repeated reuse of brines for IX resin regeneration, and optimize continuous flow reactor design to maximize brine treatment efficiency and nitrogen recovery for an economical and sustainable alternative to existing treatment operations.

Declaration of competing interest

The authors declare that they have no known competing financial interests or personal relationships that could have appeared to influence the work reported in this paper.

Acknowledgements

Financial support for this project was provided by the National Science Foundation (CBET-1804513). The authors would like to thank Pete Vicario at City of Chino for providing the waste IX brine. The authors would also like to thank BHA Altair, LLC for providing membranes for this research.

Appendix A. Supplementary data

Supplementary data to this article can be found online at https://doi.org/10.1016/j.watres.2020.115688.

References

Abdelrahman, O.A., Luo, H.Y., Heyden, A., Roman-Leshkov, Y., Bond, J.Q., 2015. Toward rational design of stable, supported metal catalysts for aqueous-phase processing: insights from the hydrogenation of levulinic acid. J. Catal. 329, 10–21.

Ahn, Y.T., Hwang, Y.H., Shin, H.S., 2011. Application of PTFE membrane for ammonia removal in a membrane contactor. Water Sci. Technol. 63 (12), 2944–2948.

Amaral, M.C.S., Magalhães, N.C., Moravia, W.G., Ferreira, C.D., 2016. Ammonia recovery from landfill leachate using hydrophobic membrane contactors. Water Sci. Technol. 74 (9), 2177–2184.

Angeles-Wedler, D., Mackenzie, K., Kopinke, F.-D., 2008. Permanganate oxidation of sulfur compounds to prevent poisoning of Pd catalysts in water treatment processes. Environ. Sci. Technol. 42 (15), 5734–5739.

Arogo, J., Zhang, R.H., Riskowski, G.L., Christianson, L.L., Day, D.L., 1999. Mass transfer coefficient of ammonia in liquid swine manure and aqueous solutions. J. Agric. Eng. Res. 73 (1), 77–86.

Bae, B.-U., Jung, Y.-H., Han, W.-W., Shin, H.-S., 2002. Improved brine recycling during nitrate removal using ion exchange. Water Res. 36 (13), 3330–3340.

Bennett, C.O., Myers, J.E., 1983. Momentum, Heat, and Mass Transfer, third ed. McGraw-Hill, Inc., New York.

Bergquist, A.M., Bertoch, M., Gildert, G., Strathmann, T.J., Werth, C.J., 2017a. Catalytic denitrification in a trickle bed reactor: ion exchange waste brine treatment. J. Am. Water Works Assoc. 109 (5), E129–E151.

Bergquist, A.M., Bertoch, M., Gildert, G., Strathmann, T.J., Werth, C.J., 2017b. Catalytic denitrification in a trickle bed reactor: ion exchange waste brine treatment. J. Am. Water Works Assoc. 109 (5), E129–E143.

Bergquist, A.M., Choe, J.K., Strathmann, T.J., Werth, C.J., 2016. Evaluation of a hybrid ion exchange-catalyst treatment technology for nitrate removal from drinking water. Water Res. 96, 177–187.

Bower, C.E., Bidwell, J.P., 1978. Ionization of ammonia in seawater: effects of temperature, pH, and salinity. J. Fish. Res. Board Can. 35 (7), 1012–1016.

Camargo, J.A., Alonso, Á., 2006. Ecological and toxicological effects of inorganic nitrogen pollution in aquatic ecosystems: a global assessment. Environ. Int. 32 (6), 831–849.

Chaplin, B., Shapley, J., Werth, C., 2009. The selectivity and sustainability of a Pd–In/γ-Al_2O_3 catalyst in a packed-bed reactor: the effect of solution composition. Catal. Lett. 130 (1–2), 56–62.

Chaplin, B.P., Roundy, E., Guy, K.A., Shapley, J.R., Werth, C.J., 2006. Effects of natural water ions and humic acid on catalytic nitrate reduction kinetics using an alumina supported Pd–Cu catalyst. Environ. Sci. Technol. 40 (9), 3075–3081.

Chen, G., Hanukovich, S., Chebeir, M., Christopher, P., Liu, H., 2019. Nitrate removal via a formate radical-induced photochemical process. Environ. Sci. Technol. 53 (1), 316–324.

Chen, H., Xu, Z., Wan, H., Zheng, J., Yin, D., Zheng, S., 2010. Aqueous bromate reduction by catalytic hydrogenation over Pd/Al_2O_3 catalysts. Appl. Catal. B Environ. 96 (3–4), 307–313.

Chen, X., Huo, X., Liu, J., Wang, Y., Werth, C.J., Strathmann, T.J., 2017. Exploring beyond palladium: catalytic reduction of aqueous oxyanion pollutants with alternative platinum group metals and new mechanistic implications. Chem. Eng. J. 313, 745–752.

Chen, Y.-X., Zhang, Y., Chen, G.-H., 2003. Appropriate conditions or maximizing catalytic reduction efficiency of nitrate into nitrogen gas in groundwater. Water Res. 37 (10), 2489–2495.

Chiueh, P.T., Lee, Y.H., Su, C.Y., Lo, S.L., 2011. Assessing the environmental impact of five Pd-based catalytic technologies in removing of nitrates. J. Hazard Mater. 192 (2), 837–845.

Choe, J.K., Bergquist, A.M., Jeong, S., Guest, J.S., Werth, C.J., Strathmann, T.J., 2015. Performance and life cycle environmental benefits of recycling spent ion exchange brines by catalytic treatment of nitrate. Water Res. 80, 267–280, 0.

Choe, J.K., Mehnert, M.H., Guest, J.S., Strathmann, T.J., Werth, C.J., 2013. Comparative assessment of the environmental sustainability of existing and emerging perchlorate treatment technologies for drinking water. Environ. Sci. Technol. 47 (9), 4644–4652.

Constantinou, C.L., Costa, C.N., Efstathiou, A.M., 2006. The remarkable effect of oxygen on the N_2 selectivity of water catalytic denitrification by hydrogen. Environ. Sci. Technol. 41 (3), 950–956.

Darestani, M., Haigh, V., Couperthwaite, S.J., Millar, G.J., Nghiem, L.D., 2017. Hollow fibre membrane contactors for ammonia recovery: current status and future developments. J. Environ. Chem. Eng. 5 (2), 1349–1359.

Ding, Z., Liu, L., Li, Z., Ma, R., Yang, Z., 2006. Experimental study of ammonia removal from water by membrane distillation (MD): the comparison of three configurations. J. Membr. Sci. 286 (1–2), 93–103.

Dortsiou, M., Katsounaros, I., Polatides, C., Kyriacou, G., 2009. Electrochemical removal of nitrate from the spent regenerant solution of the ion exchange. Desalination 248 (1–3), 923–930.

Doudrick, K., Yang, T., Hristovski, K., Westerhoff, P., 2013. Photocatalytic nitrate reduction in water: managing the hole scavenger and reaction by-product selectivity. Appl. Catal. B Environ. 136, 40–47.

du Preez, J., Norddahl, B., Christensen, K., 2005. The BIOREK® concept: a hybrid membrane bioreactor concept for very strong wastewater. Desalination 183 (1–3), 407–415.

El-Bourawi, M.S., Khayet, M., Ma, R., Ding, Z., Li, Z., Zhang, X., 2007. Application of vacuum membrane distillation for ammonia removal. J. Membr. Sci. 301 (1–2), 200–209.

Epron, F., Gauthard, F., Barbier, J., 2002. Catalytic reduction of nitrate in water on a monometallic Pd/CeO_2 catalyst. J. Catal. 206 (2), 363–367.

Garcia-González, M.C., Vanotti, M.B., 2015. Recovery of ammonia from swine manure using gas-permeable membranes: effect of waste strength and pH. Waste Manag. 38, 455–461.

Garcia-Segura, S., Lanzarini-Lopes, M., Hristovski, K., Westerhoff, P., 2018. Electrocatalytic reduction of nitrate: fundamentals to full-scale water treatment applications. Appl. Catal. B Environ. 236, 546–568.

Hörold, S., Tacke, T., Vorlop, K.D., 1993. Catalytical removal of nitrate and nitrite from drinking water: 1. Screening for hydrogenation catalysts and influence of reaction conditions on activity and selectivity. Environ. Technol. 14 (10), 931–939.

Huo, X., Van Hoomissen, D.J., Liu, J., Vyas, S., Strathmann, T.J., 2017. Hydrogenation of aqueous nitrate and nitrite with ruthenium catalysts. Appl. Catal. B Environ. 211, 188–198.

Hutchison, J.M., Guest, J.S., Zilles, J.L., 2017. Evaluating the development of biocatalytic technology for the targeted removal of perchlorate from drinking water. Environ. Sci. Technol.

Jensen, V.B., Darby, J.L., 2016. Brine disposal options for small systems in California's central valley. J. Am. Water Works Assoc. 108 (5), E276–E289.

Jung, S., Bae, S., Lee, W., 2014. Development of Pd–Cu/hematite catalyst for selective nitrate reduction. Environ. Sci. Technol. 48 (16), 9651–9658.

Kapoor, A., Viraraghavan, T., 1997. Nitrate removal from drinking water - Review. J. Environ. Eng. ASCE 123 (4), 371–380.

Kim, Y.-N., Kim, M.Y., Choi, M., 2016. Synergistic integration of catalysis and ion-exchange for highly selective reduction of nitrate into N2. Chem. Eng. J. 289, 423–432.

Lauterböck, B., Moder, K., Germ, T., Fuchs, W., 2013. Impact of characteristic membrane parameters on the transfer rate of ammonia in membrane contactor application. Separ. Purif. Technol. 116, 327–334.

Li, Y., Tarpeh, W.A., Nelson, K.L., Strathmann, T.J., 2018. Quantitative evaluation of an integrated system for valorization of wastewater algae as bio-oil, fuel gas, and fertilizer products. Environ. Sci. Technol. 52 (21), 12717–12727.

Liu, J., Choe, J.K., Wang, Y., Shapley, J.R., Werth, C.J., Strathmann, T.J., 2014. Bio-inspired complex-nanoparticle hybrid catalyst system for aqueous perchlorate reduction: rhenium speciation and its Influence on catalyst activity. ACS Catal. 511–522.

Martínez, J., Ortiz, A., Ortiz, I., 2017. State-of-the-art and perspectives of the catalytic and electrocatalytic reduction of aqueous nitrates. Appl. Catal. B Environ. 207 (Suppl. C), 42–59.

McAdam, E.J., Judd, S.J., 2008. Biological treatment of ion-exchange brine regenerant for re-use: a review. Separ. Purif. Technol. 62 (2), 264–272.

Mellor, R.B., Ronnenberg, J., Campbell, W.H., Diekmann, S., 1992. Reduction of nitrate and nitrite in water by immobilized enzymes. Nature 355 (6362), 717–719.

Mendow, G., Marchesini, F.A., Miró, E.E., Querini, C.A., 2011. Evaluation of Pd–In supported catalysts for water nitrate abatement in a fixed-bed continuous

reactor. Ind. Eng. Chem. Res. 50 (4), 1911–1920.
Moyer, B.A., Meyer, T.J., 1979. Reduction of nitrate ion by (bpy)2pyRu(OH2)2+. J. Am. Chem. Soc. 101 (5), 1326–1328.
Ngo, D.T., Sooknoi, T., Resasco, D.E., 2018. Improving stability of cyclopentanone aldol condensation MgO-based catalysts by surface hydrophobization with organosilanes. Appl. Catal. B Environ. 237, 835–843.
Nijhuis, T.A., Beers, A.E.W., Kapteijn, F., Moulijn, J.A., 2002. Water removal by reactive stripping for a solid-acid catalyzed esterification in a monolithic reactor. Chem. Eng. Sci. 57 (9), 1627–1632.
Papa, F., Balint, I., Negrila, C., Olaru, E.A., Zgura, I., Bradu, C., 2014. Supported Pd-Cu nanoparticles for water phase reduction of nitrates. Influence of the support and of the pH conditions. Ind. Eng. Chem. Res. 53 (49), 19094–19103.
Pintar, A., Batista, J., Levec, J., 2001. Integrated ion exchange/catalytic process for efficient removal of nitrates from drinking water. Chem. Eng. Sci. 56 (4), 1551–1559.
Pintar, A., Batista, J., Levec, J., Kajiuchi, T., 1996. Kinetics of the catalytic liquid-phase hydrogenation of aqueous nitrate solutions. Appl. Catal. B Environ. 11 (1), 81–98.
Pintar, A., vetinc, M., Levec, J., 1998. Hardness and salt effects on catalytic hydrogenation of aqueous nitrate solutions. J. Catal. 174 (1), 72–87.
Qi, Z., Cussler, E.L., 1985. Microporous hollow fibers for gas absorption: II. Mass transfer across the membrane. J. Membr. Sci. 23 (3), 333–345.
Qu, D., Sun, D., Wang, H., Yun, Y., 2013. Experimental study of ammonia removal from water by modified direct contact membrane distillation. Desalination 326, 135–140.
Rao, K.K., Gravelle, M., Valente, J.S., Figueras, F., 1998. Activation of Mg–Al hydrotalcite catalysts for aldol condensation reactions. J. Catal. 173 (1), 115–121.
Ruppert, A.M., Parvulescu, A.N., Arias, M., Hausoul, P.J.C., Bruijnincx, P.C.A., Gebbink, R.J.M.K., Weckhuysen, B.M., 2009. Synthesis of long alkyl chain ethers through direct etherification of biomass-based alcohols with 1-octene over heterogeneous acid catalysts. J. Catal. 268 (2), 251–259.
Sá, J., Vinek, H., 2005. Catalytic hydrogenation of nitrates in water over a bimetallic catalyst. Appl. Catal. B Environ. 57 (4), 247–256.
Soares, O.S.G.P., Fan, X., Órfão, J.J.M., Lapkin, A.A., Pereira, M.F.R., 2012. Kinetic modeling of nitrate reduction catalyzed by Pd–Cu supported on carbon nanotubes. Ind. Eng. Chem. Res. 51 (13), 4854–4860.
Tadepalli, S., Qian, D., Lawal, A., 2007. Comparison of performance of microreactor and semi-batch reactor for catalytic hydrogenation of o-nitroanisole. Catal. Today 125 (1), 64–73.
Tao, W., Ukwuani, A.T., 2015. Coupling thermal stripping and acid absorption for ammonia recovery from dairy manure: ammonia volatilization kinetics and effects of temperature, pH and dissolved solids content. Chem. Eng. J. 280 (Suppl. C), 188–196.
Tijing, L.D., Woo, Y.C., Choi, J.-S., Lee, S., Kim, S.-H., Shon, H.K., 2015. Fouling and its control in membrane distillation—a review. J. Membr. Sci. 475, 215–244.
Vardon, D.R., Settle, A.E., Vorotnikov, V., Menart, M.J., Eaton, T.R., Unocic, K.A., Steirer, K.X., Wood, K.N., Cleveland, N.S., Moyer, K.E., Michener, W.E., Beckham, G.T., 2017. Ru-Sn/AC for the aqueous-phase reduction of succinic acid to 1,4-butanediol under continuous process conditions. ACS Catal. 7 (9), 6207–6219.
Wang, L., Chen, A.S., Wang, A., Condit, W.E., Battelle, C., Sorg, T.J., Supply, W., 2011. Arsenic and Nitrate Removal from Drinking Water by Ion Exchange: US EPA Demonstration Project at Vale, OR. Final Performance Evaluation Report. National Risk Management Research Laboratory, Cincinnati, Ohio.
Wang, Y., Liu, J., Wang, P., Werth, C.J., Strathmann, T.J., 2014. Palladium nanoparticles encapsulated in core–shell silica: a structured hydrogenation catalyst with enhanced activity for reduction of oxyanion water pollutants. ACS Catal. 4 (10), 3551–3559.
Wang, Y., Qu, J., Wu, R., Lei, P., 2006. The electrocatalytic reduction of nitrate in water on Pd/Sn-modified activated carbon fiber electrode. Water Res. 40 (6), 1224–1232.
Wang, Y., Sakamoto, Y., Kamiya, Y., 2009. Remediation of actual groundwater polluted with nitrate by the catalytic reduction over copper–palladium supported on active carbon. Appl. Catal. Gen. 361 (1–2), 123–129.
Warsinger, D.M., Swaminathan, J., Guillen-Burrieza, E., Arafat, H.A., Lienhard, V., J, H., 2015. Scaling and fouling in membrane distillation for desalination applications: a review. Desalination 356, 294–313.
World Sulphuric Acid Weekly, 2017, 25 January. www.icis.com.
Wu, C., Yan, H., Li, Z., Lu, X., 2016. Ammonia recovery from high concentration wastewater of soda ash industry with membrane distillation process. Desalination Water Treat. 57 (15), 6792–6800.
Xie, Y., Cao, H., Li, Y., Zhang, Y., Crittenden, J.C., 2011. Highly selective PdCu/amorphous silica–alumina (ASA) catalysts for groundwater denitration. Environ. Sci. Technol. 45 (9), 4066–4072.
Xie, Z., Duong, T., Hoang, M., Nguyen, C., Bolto, B., 2009. Ammonia removal by sweep gas membrane distillation. Water Res. 43 (6), 1693–1699.
Yang, G.C.C., Lee, H.-L., 2005. Chemical reduction of nitrate by nanosized iron: kinetics and pathways. Water Res. 39 (5), 884–894.
Yang, T., Doudrick, K., Westerhoff, P., 2013. Photocatalytic reduction of nitrate using titanium dioxide for regeneration of ion exchange brine. Water Res. 47 (3), 1299–1307.
Ye, T., Durkin, D.P., Banek, N.A., Wagner, M.J., Shuai, D., 2017. Graphitic carbon nitride supported uUltrafine Pd and Pd–Cu catalysts: enhanced reactivity, selectivity, and longevity for nitrite and nitrate hydrogenation. ACS Appl. Mater. Interfaces 9 (33), 27421–27426.
Zarebska, A., Nieto, D.R., Christensen, K.V., Norddahl, B., 2014. Ammonia recovery from agricultural wastes by membrane distillation: fouling characterization and mechanism. Water Res. 56, 1–10.
Zhu, Z., Hao, Z., Shen, Z., Chen, J., 2005. Modified modeling of the effect of pH and viscosity on the mass transfer in hydrophobic hollow fiber membrane contactors. J. Membr. Sci. 250 (1), 269–276.